

## Driver mutations in *GNAQ* and *GNA11* genes as potential targets for precision immunotherapy in uveal melanoma patients

Sandra García-Mulero<sup>a,b,\*</sup>, Roberto Fornelino<sup>a,\*</sup>, Marco Punta<sup>c</sup>, Stefano Lise<sup>c</sup>, Mar Varela<sup>d</sup>, Luis P. del Carpio<sup>e</sup>, Rafael Moreno<sup>e</sup>, Marcel Costa-García<sup>e</sup>, Dietmar Rieder<sup>f</sup>, Zlatko Trajanoski<sup>f</sup>, Alena Gros<sup>g</sup>, Ramón Alemany<sup>e</sup>, Josep María Piulats<sup>h</sup>, and Rebeca Sanz-Pamplona<sup>a,i</sup>

<sup>a</sup>Unit of Biomarkers and Susceptibility, Oncology Data Analytics Program (ODAP), Catalan Institute of Oncology (ICO), Oncobell Program, Bellvitge Biomedical Research Institute (IDIBELL) and CIBERESP, Barcelona, Spain; <sup>b</sup>Anatomy Unit, Department of Pathology and Experimental Therapy, and Department of Clinical Sciences, Faculty of Medicine and Health Sciences, University of Barcelona, Barcelona, Spain; <sup>c</sup>Bioinformatics Core, Centre for Evolution and Cancer, The Institute of Cancer Research, London, UK; <sup>d</sup>Department of Pathology, Bellvitge University Hospital, Barcelona, Spain; <sup>e</sup>Procure Program, Catalan Institute of Oncology (ICO), Oncobell Program, Bellvitge Biomedical Research Institute (IDIBELL), Barcelona, Spain; <sup>f</sup>Institute of Bioinformatics, Biocenter, Medical University of Innsbruck, Innsbruck, Austria; <sup>g</sup>Tumor Immunology and Immunotherapy, Vall d'Hebron Institute of Oncology (VHIO), Barcelona, Spain; <sup>h</sup>Department of Medical Oncology, ICO, IDIBELL and CIBERONC, Barcelona, Spain; <sup>i</sup>Institute for Health Research Aragon (IISA), ARAID Foundation, Aragon Government, University Hospital Lozano Blesa, Zaragoza, Spain

### ABSTRACT

Uveal melanoma (UM) is the most common ocular malignancy in adults. Nearly 95% of UM patients carry the mutually exclusive mutations in the homologous genes *GNAQ* (amino acid change Q209L/Q209P) and *GNA11* (amino acid change Q209L). UM is located in an immunosuppressed organ and does not suffer immunoeediting. Therefore, we hypothesize that driver mutations in *GNAQ/11* genes could be recognized by the immune system. Genomic and transcriptomic data from primary uveal tumors were collected from the TCGA-UM dataset ( $n = 80$ ) and used to assess the immunogenic potential for *GNAQ/GNA11* Q209L/Q209P mutations using a variety of tools and HLA type information. All prediction tools showed stronger *GNAQ/11* Q209L binding to HLA than *GNAQ/11* Q209P. The immunogenicity analysis revealed that Q209L is likely to be presented by more than 73% of individuals in 1000 G databases whereas Q209P is only predicted to be presented in 24% of individuals. *GNAQ/11* Q209L showed a higher likelihood to be presented by HLA-I molecules than almost all driver mutations analyzed. Finally, samples carrying Q209L had a higher immune-reactive phenotype. Regarding cancer risk, seven HLA genotypes with low Q209L affinity show higher frequency in uveal melanoma patients than in the general population. However, no clear association was found between any HLA genotype and survival. Results suggest a high potential immunogenicity of the *GNAQ/11* Q209L variant that could allow the generation of novel therapeutic tools to treat UM like neoantigen vaccinations.

### ARTICLE HISTORY

Received 19 April 2023  
Revised 27 August 2023  
Accepted 17 September 2023

### KEYWORDS

*GNA11*; *GNAQ*; HLA; immunotherapy; neoantigen; uveal melanoma

## 1. Introduction


Despite being considered a rare tumor (10 cases per million in Europe), uveal melanoma (UM) is the most common ocular malignancy in adults.<sup>1</sup> Prognosis is still poor, with up to 50% of patients developing metastasis, mostly in the liver. Metastatic UM does not have an effective standard treatment available. Although survival rates have not improved significantly in the last decades,<sup>2</sup> a recent study showing for the first time a certain survival advantage in patients treated with Tebentafusp is worth mentioning. This is a novel kind of molecule consisting of soluble TCR against gp100 expressed in HLA-A\*02:01 and a lymphocyte activating domain (CD3). Unfortunately, only 40–50% of the European population express HLA-A\*02:01, and eventually, almost all the patients treated with tebentafusp

presented disease progression.<sup>3,4</sup> Thus, there is a need for active treatments.

At the molecular level, UM is very different from cutaneous melanoma. Both arise from melanocytes, but they do not share somatic mutations driving carcinogenesis. Indeed, UM shows exclusive mutations in the *GNA* gene family. Nearly 95% of UM patients carry the mutually exclusive mutations *GNAQ/GNA11* in the hotspot Q209. These mutations change the conserved catalytic glutamine, Q, for a Proline, P, or Leucine, L, leading to the constitutive activation of the GTPase domain.<sup>5</sup> These oncogenic mutations in G protein-coupled receptor (GPCR) activate pathways including MPAK, PI3K/AKT or YAP/TAZ promoting tumor progression<sup>6</sup>. After the *GNAQ/GNA11* mutation, a second driver event is necessary for

**CONTACT** Rebeca Sanz-Pamplona  [rsanz@iisaragon.es](mailto:rsanz@iisaragon.es)  Institute for Health Research Aragon (IISA), ARAID Foundation, Aragon Government, University Hospital Lozano Blesa, San Juan Bosco 15, Zaragoza 50009, Spain; Josep María Piulats  [jmpiulats@iconcologia.net](mailto:jmpiulats@iconcologia.net)  Department of Medical Oncology, ICO, IDIBELL and CIBERONC, L'Hospitalet de Llobregat, Hospital Duran i Reynals, Avinguda de la Granvia de l'Hospitalet, 199-203, Barcelona 08908, Spain

\*both authors contribute equally to this work.

 Supplemental data for this article can be accessed online at <https://doi.org/10.1080/2162402X.2023.2261278>

© 2023 IDIBELL. Published with license by Taylor & Francis Group, LLC.

This is an Open Access article distributed under the terms of the Creative Commons Attribution-NonCommercial License (<http://creativecommons.org/licenses/by-nc/4.0/>), which permits unrestricted non-commercial use, distribution, and reproduction in any medium, provided the original work is properly cited. The terms on which this article has been published allow the posting of the Accepted Manuscript in a repository by the author(s) or with their consent.

malignant transformation. The premalignant cells either present loss of function BAP1 or mutations in SF3B1 or EIF1AX. This second hit also occurs in a mutually exclusive fashion.<sup>7</sup>

Unlike cutaneous melanoma, responses to immune checkpoint inhibitors are much less common in UM patients.<sup>8,9</sup> This could be due to several molecular and anatomical differences. UM is located in an immune-privileged organ, protected by the blood-ocular barrier, and exhibits an immunosuppressive microenvironment. Because of that, it does not suffer immunoediting.<sup>10</sup> Moreover, the tumor mutational burden (TMB) is very high in cutaneous melanoma but low in UM.<sup>11</sup> Thus, UM generates low levels of neoantigens and is considered a tumor with low antigenicity.<sup>5</sup> Also, we and others showed that immune cell infiltration is associated with poor prognosis in UM.<sup>12-14</sup>

Although driver mutations are normally cataloged as non-immunogenic, recent work supports the possibility to develop immunotherapeutic drugs against neoantigens derived from recurrent mutations in cancer driver genes.<sup>15</sup> In this regard, we hypothesize that recurrent mutations in GNAQ and GNA11 genes could elicit T-cell responses. Given the predicted low immune selective pressure in UM, it could represent an attractive target for immunotherapeutic interventions. Also, we hypothesize that different mutations (Q209P or Q209L) could have different antigenicity and response from the immune system. Our objective is to computationally analyze the antigenicity of tumors harboring GNAQ/11 mutations, characterize their microenvironment, and assess their association with clinical phenotypes. Our results suggest that the Q209L mutation is more immunogenic than the Q209P mutation, irrespectively of the mutated gene (GNAQ or GNA11).

## 2. Methods

### 2.1. Samples

Clinical and mutational data of paired primary uveal tumors and blood samples from patients were collected from the TCGA-UM dataset ( $n = 80$  pairs). Annotated mutational data were downloaded from the cBioPortal.<sup>16</sup> RNA-seq was downloaded in fragments per kilobase per million (FPKM) and then converted to log<sub>2</sub> scale. Supplementary Table S1 includes a detailed description of patients included in the dataset. Comparison between groups was performed using the chi-squared test for categorical variables and the Wilcoxon test for numerical variables. For survival analysis, a series of 147 primary uveal melanoma samples from University Hospital of Bellvitge (named Bellvitge clinical dataset) with clinical and mutational status information was used (Supplementary Table S2). The study was approved by the local ethical committee.

### 2.2. Immunogenicity prediction of neoantigens GNAQ-L, GNAQ-P and GNA11-L

First, for each mutation, 17 mers amino acid sequences with the mutated amino in the middle were constructed using an in-house script. Wild-type sequences were also generated. The immunogenic potential for GNAQ-L, GNAQ-P and GNA11-L was assessed in a variety of binding prediction tools

(NetMHC,<sup>17</sup> NetMHCpan,<sup>18</sup> NetMHCcons,<sup>19</sup> NetMHCpanstab<sup>18</sup> MHCSeqNet<sup>20</sup> and MHCflurry<sup>21</sup> using HLA supertypes and all nine mer combinations from the two mutated sequences as input.<sup>18-25</sup> All prediction tools but NetMHCstabpan score the affinity of the inputted peptides for a specific HLA. NetMHCstabpan calculates a combined score for the affinity but also the stability of the binding. The outputs of the different tools were diverse. The NetMHC tools and MHCflurry calculate the affinity value measured in nM, which is used to filter the binders or no binders. These affinity values are also shown as logarithmic transformations, called % Rank. Only the nine mers with a %Rank equal to or below 2 were considered binders. On the other hand, the output of MHCSeqNet is a probability value between 0.0 and 1.0, where 0.0 refers to a non-binder and 1.0 to a strong binder. Only those with more than a 60% probability of binding were taken. Lastly, MixMHCpred does not provide affinity values; instead, it calculates a Score and a %Rank value for each HLA allele. For a single allele, scores larger than 0 correspond to % a rank smaller than 1%. Therefore, in the case of this tool, the nine mers in which the best allele score is higher than 0 were chosen as binders.

Apart from solo binding prediction, the NetCTL tool was used to predict proteasomal C terminal cleavage and TAP transport efficiency.<sup>26</sup> The proteasome cleavage event is predicted using the version of the NetChop neural networks trained on C terminals of known CTL epitopes as described for the NetChop-3.0 server.<sup>27</sup> The TAP transport efficiency is predicted using the weight matrix-based method described by Peters et al.<sup>26</sup> NetCTL predicts MHC peptide binding using neural networks in NetMHC server and then calculates a combined score for the three measures. As an input, fasta files with GNAQ and GNA11 protein sequences were used. Affinity and MS data used to train NetMHC were used for motif deconvolution of FRMVDVGGL peptide.

### 2.3. HLA presentation scores

All HLA-presentation scores were defined starting from eluted ligand likelihood percentile ranks of peptides with respect to HLA allotypes obtained from the NetMHCpan-4.0 prediction method.<sup>18</sup> NetMHCpanI were run (HLA type I only predictions) on all neopeptides of length 8 to 11 generated by each of the three mutations (GNAQ-L, GNAQ-P, and GNA11-L) against a set of 195 HLA(-A/-B/-C) types found in the > 1,000 individuals of the 1000 Genomes project (1000 G).<sup>28</sup> Nineteen mer amino acid sequences were used. For each individual, there was information about six HLA types.

Each mutation was mapped to a protein sequence and associated to a set of 38 mutated peptides using an in-house Python script to generate all possible peptides of lengths 8 to 11 that spanned the mutation. A wild-type peptide was associated with each specific mutant peptide that was identical to the mutant peptide except that the mutated amino acid is reverted to the wild-type one. For each peptide in this set, the program NetMHCpan-4.0 was used to calculate the eluted ligand likelihood percentile rank and predict the interaction core peptide (Icore) with respect to all HLA allotypes. The elution rank

takes values in the range from 0 to 100, with lower values representing higher presentation likelihoods. We defined the presentation score of a mutation with respect to a specific HLA allotype as the minimum elution rank among all associated peptides but excluding those with a wild-type Icore. We called this presentation the BR score.

PHBR score (Patient Harmonic-Mean Best Rank) was calculated by combining the six best rank scores of the six HLA allotypes using a harmonic mean. Also, we calculated our Population-Wide Median Harmonic-Mean Best Rank (PMHBR) as the median of the PHBR scores of a mutation calculated over a set of individuals. Lower PMHBR scores correspond to higher likelihood for the mutation to be presented across our 1000 G or TCGA populations.<sup>29</sup>

#### 2.4. HLA frequency analysis

Whole-exome sequencing raw data were used to infer HLA genotypes in the uveal melanoma samples using Optitype software.<sup>30</sup> Frequencies of HLA alleles within the uveal melanoma population were calculated and compared with 1000 G HLA frequencies using a Binomial test. Differences were considered significant when adjusted p-value <0.05.

#### 2.5. Immune microenvironment characterization

The immune microenvironment of the samples was characterized using gene expression data and a variety of bioinformatics tools. The immunophenoscore (IPS) function was used to measure the immune state of the samples by the quantification of four different immune phenotypes in a given tumor sample (Antigen Presentation, Effector Cells, Suppressor Cells, and Checkpoint markers) using gene markers. Also, it computes an aggregated z-score summarizing the four immune phenotypes.<sup>31</sup> Samples were scored using the gene set variation analysis (GSVA) method with 18 gene marker lists from ConsensusTME<sup>32</sup> and the T-cell inflammatory (TIS) signature.<sup>33</sup>

#### 2.6. Differential expression (DEG) and functional analysis

A differential expression analysis between Q209P and Q209L samples was performed with R package *Limma*. Differentially expressed genes (DEGs) were selected as those with log<sub>2</sub> fold change (log<sub>2</sub>FC) > abs(2) and adjusted p-value <0.01. To identify enrichment in specific cellular functions and pathways, a Gene Set Enrichment Analysis (GSEA) was performed using DEGs. Hallmark gene sets from MsigDB were interrogated.

#### 2.7. Survival analysis

A survival analysis was done with a cohort of patients from the Bellvitge University Hospital (*n* = 147). Univariate and multivariate Cox proportional hazard regression models were fitted to assess recurrence-free survival (RFS) and overall survival (OS) association between patients harboring Q209P and Q209L mutation. Kaplan–Meier curves were plotted to represent the results and the Log-rank test was computed. All statistical analyses were performed using with R version 3.5.0 (R Foundation for Statistical Computing, Vienna, Austria).

### 3. Results

#### 3.1. GNAQ/GNA11 mutations in TCGA-UM dataset

GNAQ and GNA11 were the genes harboring the most frequent missense mutations in TCGA-UM dataset and were mutually exclusive (Figure 1a). Out of 80 TCGA-UM patients, 34 patients carried GNA11 p.Q209L (hereafter GNA11-L), 10 patients carried GNAQ p.Q209L (hereafter GNAQ-L), and 27 patients GNAQ p.Q209P (hereafter GNAQ-P). The other nine samples were wild type at the position of interest; two patients carried GNAQ p.R183Q mutation, one more patient carried GNAQ p.G48V, one patient GNA11 p.R183C, and one patient GNA11 p.R166H. Two individuals were mutant at the same time for GNAQ and GNA11 but not in position 209 (one case at positions GNAQ p.Q209L and GNA11 p.R166H; second case at positions GNAQ p.R183Q and GNA11 p.R183C) (Figure 1b).

Despite being located in different chromosomes (Chromosome 9 and Chromosome 19, respectively), GNAQ and GNA11 genes are highly homologous and so are the resulting proteins. A BLAST alignment showed 90% identity between the two proteins (Supplementary Figure S1). GNAQ-L and GNA11-L suffered the same amino acid change in position 209 (from Q-Glutamine- to L-Leucine-) and, given the high homology between these two proteins, the resulting peptide in which the mutation is centered were identical. On the other hand, GNAQ-P changed from Q (Glutamine) to P (Proline). Because of this, and since we planned to study the potential immunogenicity of those mutations rather than protein function, we decided to compare patients harboring P mutated vs. patients harboring L mutated, irrespectively of the gene of origin (Figure 1b). In total, 71 (89%) patients carried the Q209P/L amino acid change, of which 44 (62%) carry amino acid change p.Q209L and 27 (38%) carry change p.Q209P.

To see whether there was any association between the different changes Q209P or Q209L and the different clinical variables in the dataset, we performed a statistical test by mutation change (Supplementary Table S3). No association was found with age, sex, overall survival time and status, recurrence-free survival status, recurrence, fraction of genome altered, SCNA subtype cluster, BAP1 mutation, Chromosome 3 status (disomy or monosomy), or Chromosome 8 status (disomy or polysomy). The only significant association was the mutation count (Wilcoxon test, p-value = 0.028), indicating that patients with Q209L mutations have a slightly higher number of mutations (a mean of 13.3 vs. 11.1). However, this is not significant when multitesting correction was applied.

#### 3.2. Binding affinity prediction of neoantigens GNAQ-L, GNAQ-P and GNA11-L

Two different approaches were taken to explore this issue. On the one hand, the probability of peptides containing the mutations to be presented by HLA supertypes was tested using a variety of prediction tools. On the other hand, presentation scores for GNAQ-L, GNAQ-P, and GNA11-L were calculated over all HLA genotypes in the 1000 G database.

First, the 17-length peptides for GNAQ-L/GNA11-L (Q209L) (FRMVDVGGLRSERRKW) and GNAQ-P (Q209P)

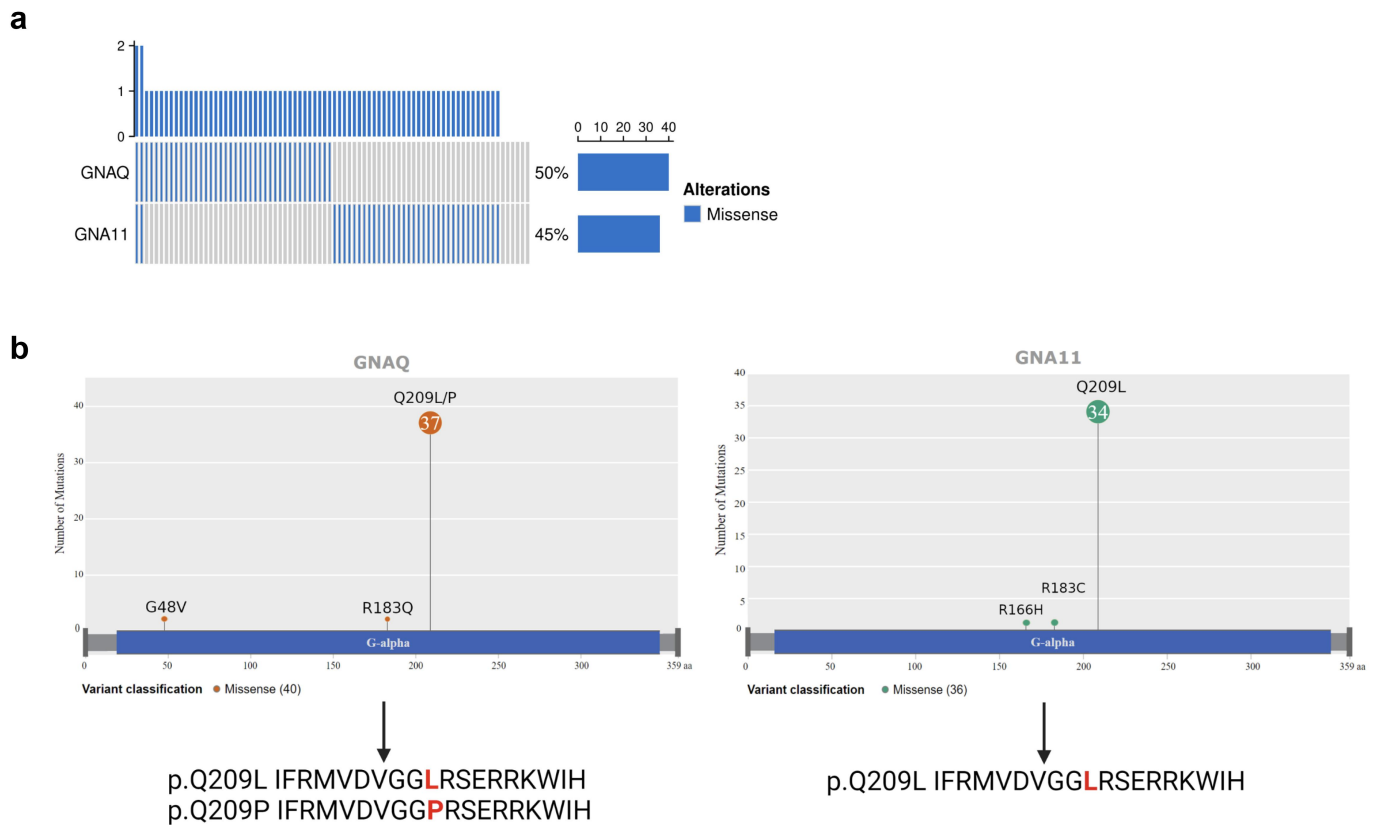


**Figure 1.** GNAQ and GNA11 mutations in TCGA UM samples. a) Mutational status of GNAQ and GNA11 genes. Bar plot shows mutated patients in blue and wild type in gray. The frequency of alterations is 50% for GNAQ and 45% for GNA11. b) Lollipop plot showing GNAQ and GNA11 mutations across the proteins and resulting peptides harboring Q209P and Q209L mutations. Amino acid changes are marked in red.

(FRMVDVGGPRSERRKWI) were used to test the antigenicity of these mutations using a total of seven different binding prediction tools, to avoid any bias related to similar Machine Learning algorithms or datasets used for the training. All methods predicted Q209L mutation as having a higher probability of presentation than Q209P, except for NetMHCpan (Figure 2). A total of 12 non-unique bindings with six HLA types were found for Q209P variant, whereas a total of 29

bindings with eight HLA alleles were found for Q209L. Moreover, none of the Q209P-derived peptides were predicted as strong binders although only four out of the seven tested tools give information about the strength of the binding. On the contrary, strong binders were found in the case of Q209L mostly with FRMVDVGGGL peptide (Table 1). The HLA alleles giving rise to strong bindings with Q209L mutation were HLA-A\*03:01, HLA-B\*27:05, and HLA-B\*39:01 (Supplementary Table S4).

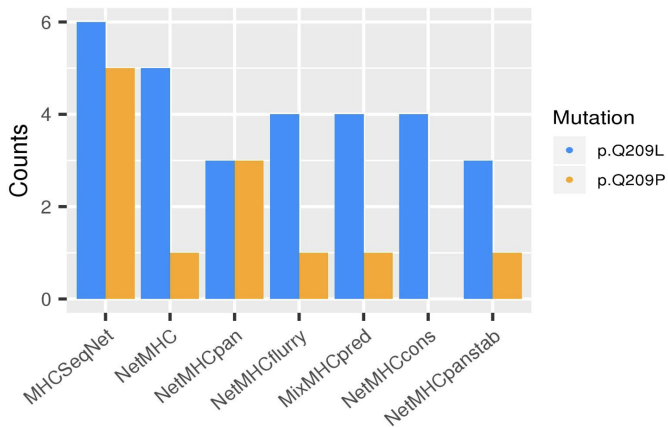


**Figure 2.** HLA-Q209L and HLA-Q209P binding prediction. Bar plot showing the number of successful bindings predicted of Q209L change (in blue) and Q209P (in orange) across seven prediction tools (in x axes), using HLA supertype genotypes.

To know if these mutations were likely to be presented by any individual from the 1000 G database, as a sample of a healthy population, we calculated how many individuals have at least one mutant peptide (length 8 to 11) that has presentation likelihood below a given threshold for at least one of the HLA types of the individual. For threshold % rank < 0.5 (Strong binding), up to 73% of individuals were predicted to present Q209L peptide, while only 24% of individuals were predicted to present Q209P peptide. Looking at threshold % rank < 2 (weak binding), 88% of individuals were presenting Q209L peptides, and 74% of individuals presented Q209P. Moreover, we generated a BR score for each sample carrying Q209L by taking the minimum BR score of all six BR per patient. A total of 69.7% of samples have at least one strong binding (BR < 0.5), while 16.3% have a weak binding (0.5 < BR) and 14% have no binding (BR > 2).

Next, the percentage rank score of mutant peptides was compared to the percentage rank of their corresponding wild-type

**Table 1.** Q209P/L–HLA type pairs binding prediction per tool. Weak binder (WB) and strong binder (SB).

Allele	NetMHC	NetMHCpan	NetMHCcons	NetMHCpanstab	MHCSeqNet	MHCflurry	MixMHCpred
HLA-A*01:01	MVDVGGLRS (WB)		MVDVGGLRS (WB)		MVDVGGLRS MVDVGGPRS		MVDVGGLRS
HLA-A*03:01	RMVDVGGLR (WB)	RMVDVGGPR (WB) RMVDVGGLR (WB)	RMVDVGGLR (WB)	RMVDVGGPR (WB) RMVDVGGLR (WB)	RMVDVGGPR RMVDVGGLR	RMVDVGGPR RMVDVGGLR	
HLA-A*26:01		DVGGPRSER (WB)					DVGGLRSER
HLA-B*07:02	GPRSERRKW (WB)	GPRSERRKW (WB)			GPRSERRKW		GPRSERRKW
HLA-B*08:01							
HLA-B*27:05	<b>FRMVDVGGL</b> (SB) <b>LSRERRKWI</b> (SB)	FRMVDVGGL (SB)	<b>FRMVDVGGL</b> (SB)	FRMVDVGGL (SB)	<b>FRMVDVGGP</b> FRMVDVGGL <b>LSRERRKWI</b>	<b>FRMVDVGGL</b> <b>LSRERRKWI</b>	
HLA-B*39:01	<b>FRMVDVGGL</b> (SB)	FRMVDVGGL (SB)	<b>FRMVDVGGL</b> (SB)	FRMVDVGGL (SB)	FRMVDVGGP <b>FRMVDVGGL</b> GLRERRKW	<b>FRMVDVGGL</b>	FRMVDVGGL
HLA-B*58:01							GLRERRKW

(WT) peptides. This may be relevant because given the similarity between WT and mutants (a single aa difference), it is possible that if the WT is presented, the mutant (even if presented) may be subjected to tolerance mechanisms and thus not be immunogenic. For % rank < 0.5 threshold, in 59% of individuals, the mutated peptide Q209L is predicted to be presented with strong binding, while the Q209L WT is not. On the other side, only 8% of individuals are predicted to present the Q209P mutated peptides and not the Q209P WT peptide. So, mutation Q209L has the most encouraging differences with respect to WT.

Finally, the HLA binding affinity was predicted through a score of antigenicity for the two mutations Q209P and Q209L. This score is calculated based on the “Best rank” score of NetMHCpanI for the 1000 G population. As explained, the BR score represents the Best Rank for each individual, while the PMHBR is the median population BR score. The PMHBR score of Q209P is 3.66, while the PMHBR score of Q209L is 0.62. Then, we compared these scores to other driver mutations, and we see that Q209L mutation

has one of the lowest scores, meaning that it has a higher likelihood to be presented across the population than most of the driver mutations of different cancer types (Figure 3).

Regarding peptides, in agreement with previous results, FRMVDVGGL emerged as the most immunogenic amino acid sequence since it scored better in 80 out of the 195 HLA alleles followed by MVDVGGLS(27), RMVDVGGL (26), GLRERRKW (24), RMVDVGGLR (19), DVGGLRSER (10), IFRMDVGGL (7), LSRERRKWI (1) and VDVGGLRSE (1). To gain insight into the immunogenicity of peptide FRMVDVGGL, a motif study was done. Figure 4 shows deconvoluted motifs obtained using affinity and MS data from NetMHCpan. In both cases, anchor residues showing best performance with HLA-C\*07:02 were R in position 2 and L in position 9 (as in FRMVDVGGL). Because of its hydrophobicity, Leucine (L) is an anchoring residue key for the affinity with the HLA molecule. On the contrary, the Proline (P) in the non-mutated peptide is not. So, it makes sense that the Q to L amino acid change turns the peptide a strong binder. In agreement, the tool netMHCstabpan predicts a higher stability for the mutated peptide in the different HLA alleles most likely due to the new anchor.

Apart from binding to HLA, for a neoantigen to be present, it needs to be processed by the proteasome and transported by the TAP mechanism. We used NetCTL to predict proteasomal C terminal cleavage and TAP transport efficiency. As a result, for Q209L, we got three putative neoantigens, whereas we got only two in the case of Q209P. For Q209L, NetCTL selected nine mer FRMVDVGGL as a good candidate to be presented by HLA-B\*27:05 and HLA-B\*39:01 and RMVDVGGLR to be presented by HLA-A\*03:01. These two peptides were also predicted to be binders by all the other tools, the former as a strong binder and the latter a weak binder.

Taking together, all these results support that Q209L mutation is more immunogenic, since it is predicted to be properly processed and presented with good affinity and stability.

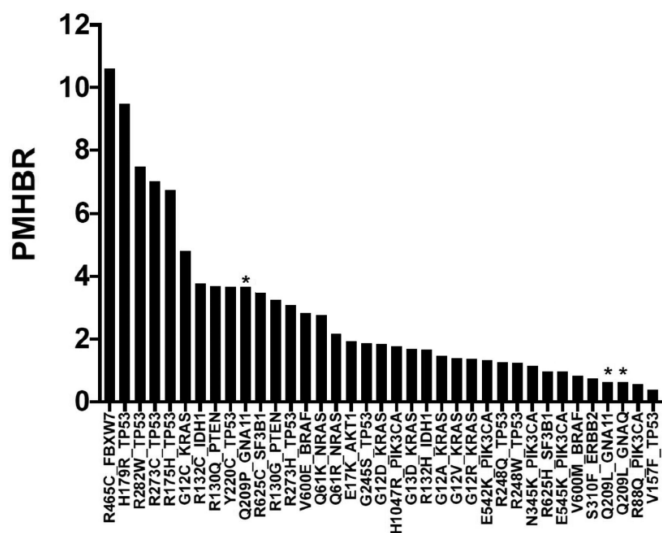


**Figure 3.** PBHBR score (patient Harmonic-mean best rank score) of a list of driver mutations across 1000 G individuals. The lower the PBHBR scores, the higher probability to be presented. Q209L shows higher likelihood to be presented by HLA molecules than Q209P and most driver mutations in cancer. Asterisks marks Q209P and Q209 L mutations.

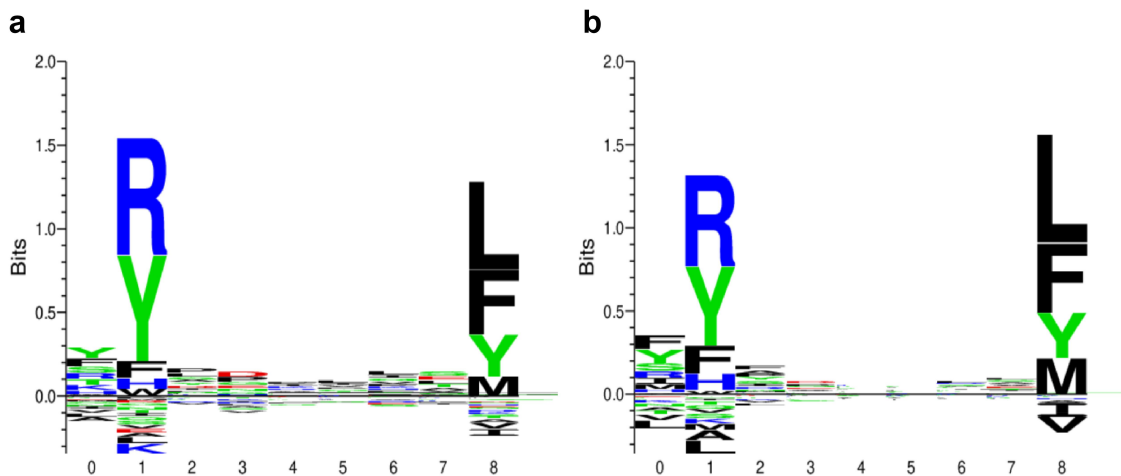


**Figure 4.** Motif deconvolution of peptide FRMVDVGGGL. Motif deconvoluted from mass spectrometry (a) and from affinity data (b) using NetMHCpan training data. In both, anchor residues showing best performance are R in position 2 and L in position 9 (numbered as 1 and 8 respectively in X axis of the plots).

### 3.3. Correlation of HLA alleles frequencies and uveal melanoma risk and survival

Next, we wanted to assess if having different HLA alleles (implying different binding affinity for Q209L) has an impact on uveal melanoma risk or survival. First, we wondered if there was a relationship between HLA haplotype frequency and the Q209L BR scores. In the general population, the BR score of Q209L mutation did not correlate with HLA frequency for HLA-A and HLA-B genes (Figure 5a), while BR score and HLA-C exhibited a non-significant trend toward a negative correlation. For UM patients, the negative correlation between HLA-C allele frequency and the BR score was stronger (Spearman correlation =  $-0.55$   $p = .029$ , Figure 5b). Results from 1000 G population pointed to HLA-C\*07:02 as the allele with a higher frequency and lower BR score. On the contrary, HLA-A\*24:02 is an example of frequent allele with no predicted binding affinity for Q209L (Figure 5c).

HLA frequencies between uveal patients and the general healthy population (1000 G) were compared by the binomial test, and the resulting frequencies were plotted in a radar plot (Figure 6a, Supplementary Table S5). As a result, 10 haplotypes showed differences at a FDR of  $< 0.05$  between uveal and population frequencies, of which nine showed higher frequency in uveal melanoma patients: HLA-A\*01:01, HLA-A\*02:01, HLA-B\*08:01, HLA-B\*15:01, HLA-B\*18:01, HLA-B\*44:02, HLA-C\*01:02, HLA-C\*05:01, HLA-C\*07:01, HLA-C\*12:03. Of those alleles, only HLA-C\*07:01 and HLA-A\*01:01 have a BR score of high antigenicity ( $BR < 2$ ). The other seven have low antigenicity scores (high BR value scores ( $BR > 2$ ), suggesting that a genetic selection in uveal melanoma patients made neoantigen Q209L hide. The same analysis was performed for comparing the HLA frequencies between patients harboring Q209L or Q209P mutations (Supplementary Figure S2). In this case, no statistical differences were found between the frequencies.

Moreover, to find out whether there could be selection toward lower antigenic binding in patients carrying the highly antigenic Q209L change and relapsing, we compared the HLA frequencies

in patients carrying Q209L mutation, between recurrent and non-recurrent uveal melanoma samples. None of the HLA haplotypes compared by binomial test showed statistically significant differences, but there was a trend toward having a higher frequency in HLA-B\*44:02, HLA-B\*07:02, and HLA-B\*18:01 in non-recurrent samples, which are three alleles with low binding affinity to Q209L (Figure 6b). Also, we wondered if HLA alleles with higher chances of presenting Q209L were absent in uveal melanoma patients. However, there were no statistically significant differences in BR score between haplotypes present and missing in uveal melanoma patients (Supplementary Figure S3).

Finally, a survival analysis was performed on a total of 147 human samples from the Bellvitge University Hospital (clinical dataset) between Q209L and Q209P patients. First, we performed a statistical test by mutation change (Supplementary Table S6) to assess differences between the two groups. No association was found with age, sex, overall survival time and status, recurrence-free survival time and status, fraction of genome altered, SCNA subtype cluster, BAP1 mutation, SF3B1 mutation, EIF1AX mutation, Chromosome 3 status (disomy or monosomy), or Chromosome 8 status (disomy or polysomy). Next, Cox models were fitted for elucidating the impact of the GNAQ/11 mutational status on outcome. In a univariate Cox proportional hazard model, Q209P mutation was associated with worse outcome, although results were not significant (Supplementary Figure S4A). Similar not statistically significant results emerged from a multivariate Cox regression analysis showing that Q209P mutated patients have a hazard ratio of 1.48 in comparison with Q209L mutated patients (Supplementary Table S7). Kaplan–Meier curves in Supplementary Figure S4B showed Q209L patients having slightly better recurrence-free survival (RFS) than Q209P patients (Log-rank test  $p = .13$ ). An interesting observation is that three out of the 147 patients were metastatic at the time of diagnosis. All these three tumors harbor the Q209P mutation, pointing to a more aggressive phenotype. Unfortunately, it is not possible to make a statistical analysis because of the low

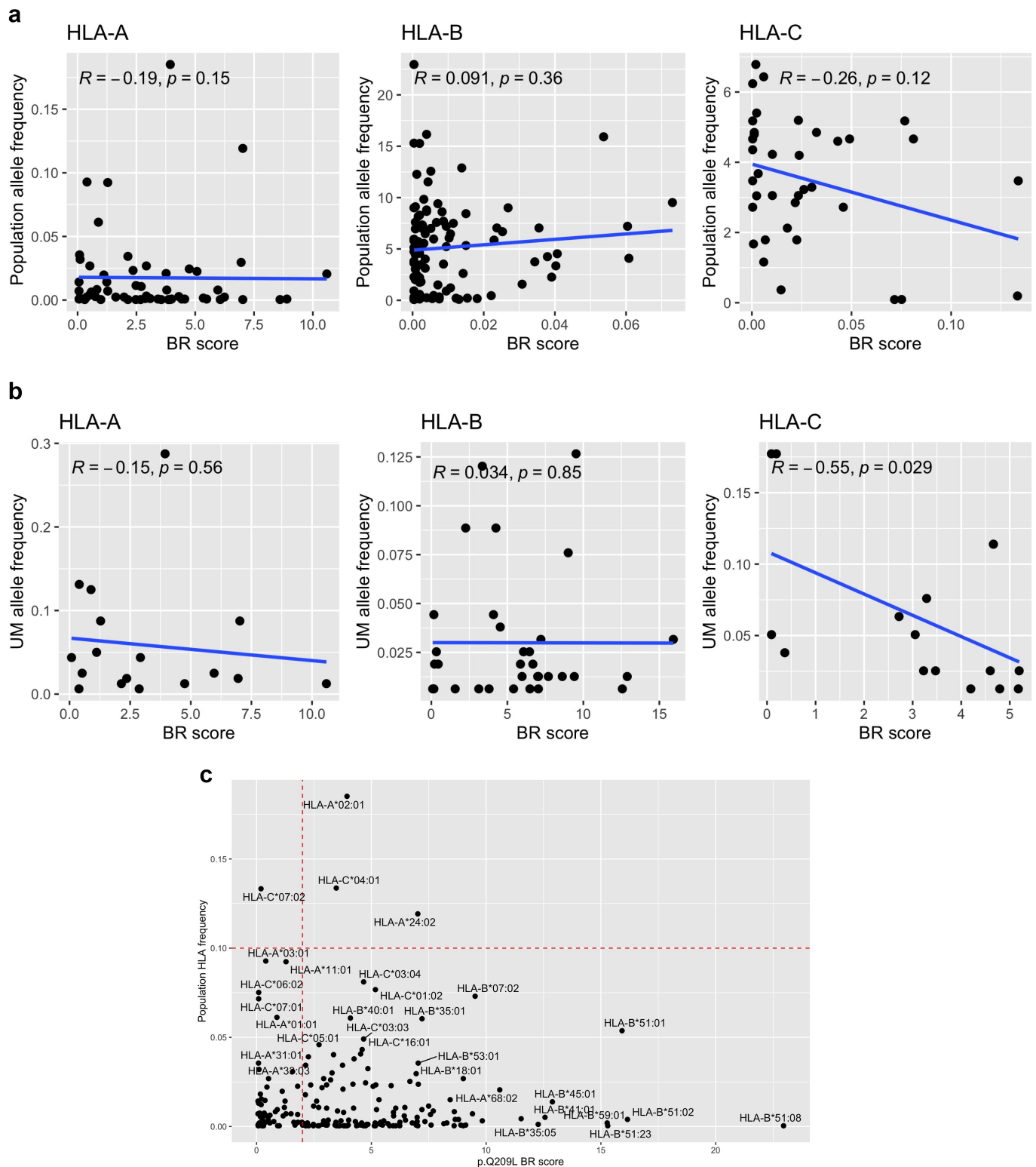


**Figure 5.** Correlation between presentation probability and HLA haplotypes. Plots show correlation between BR score of Q209L and the HLA-A, HLA-B and HLA-C type frequency in (a) general population and (b) in UM patients. c) Plot showing BR score for Q209L in the x-axis and population HLA frequency in the y-axis with HLA haplotypes of high frequency annotated.

number of cases. It is worth to mention that in TCGA data, we did not find any relationship between P/L mutations and prognosis.

In summary, no clear associations were found between HLA haplotypes and the risk of suffering uveal melanoma nor between HLA frequency and survival. It is important to point

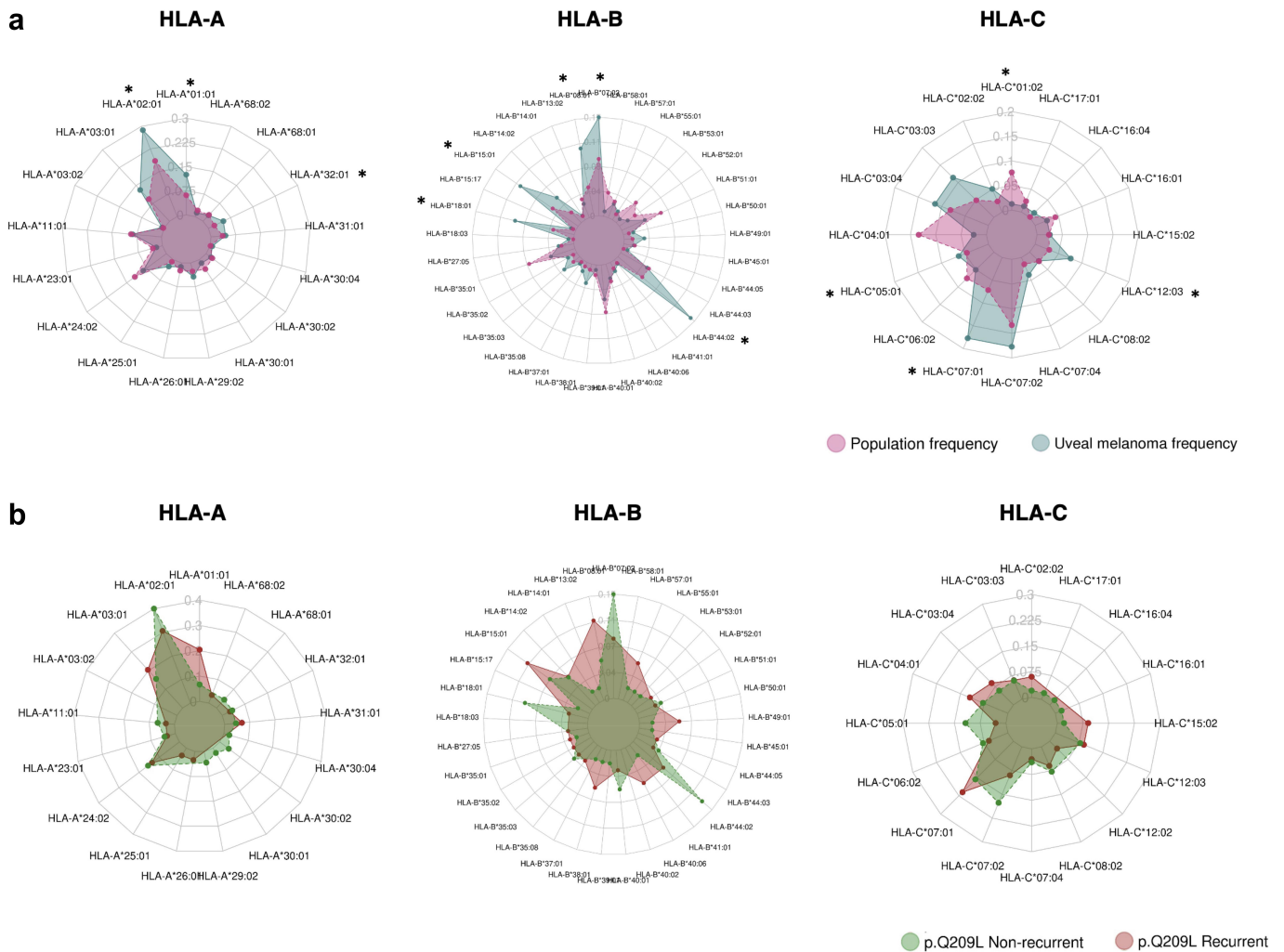


**Figure 6.** HLA frequency association with UM risk and survival. Radar plots comparing frequencies in HLA haplotype for HLA-A, HLA-B, and HLA-C genes between UM patients (green) and 1000 G individuals (purple) (a), and between recurrent (red) and non-recurrent (green) patients harboring Q209L (b). Asterisks correspond to haplotypes with statistical differences by Binomial test (FDR p-adjusted <.05). Only haplotypes which are present in uveal melanoma patients are depicted.

out that there is a possibility that we did not find statistical differences because of the low sample size.

### 3.4. GNAQ/11 Q209P/L mutations and survival, in other tumors

Q209 mutations in GNAQ/11 genes are almost but not exclusive of uveal melanoma patients. One could expect that tumors growing in non immune privileged organ harboring Q209L mutation and having an HLA with high affinity for the mutant peptide were attacked by the immune system. To explore this issue, we have mined cBioPortal looking for GNAQ/11 mutated patients across all TCGA datasets. As expected, and in line with our hypothesis, only six out of 10,887 samples from five skin melanoma patients carried Q209P/L mutations (two the Q209P mutation and three the Q209L). HLA genotypes for these skin melanoma patients were inferred and annotated with the corresponding Q209L BR scores and allelic frequency (Supplementary Figure S5). Unexpectedly, one of the Q209L mutants was a strong binder. Indeed, and in agreement, this sample appeared in TCIA portal<sup>31</sup> as the generator of a putative

neoantigen derived from GNA11. Given the large number of examined tumors, this is clearly an exception. One can speculate that this tumor has an efficient molecular mechanism to evade immune system surveillance.

### 3.5. Samples harboring GNAQ-P or GNA-L mutations showed differences in the tumor microenvironment

We used expression data from TCGA samples to characterize the immune state of samples carrying Q209L mutation or Q209P mutation. First, we evaluated whether there were differences in the levels of antigen processing and presentation genes (Figure 7a). All genes related to MHC class I showed higher gene expression in patients carrying Q209L mutation (Wilcoxon test; HLA-A,  $p = .009$ ; HLA-B,  $p = .039$ ; HLA-C,  $p = .034$ , B2M,  $p = .043$ ).

Next, we used several tools to characterize the immune system activation status of samples. The T-cell inflamed signature (TIS score) was estimated and showed no differences between Q209L and Q209P mutated patients (Figure 7b). The Immunophenoscore, which is used as global score of the immune state of the samples, was significantly higher in



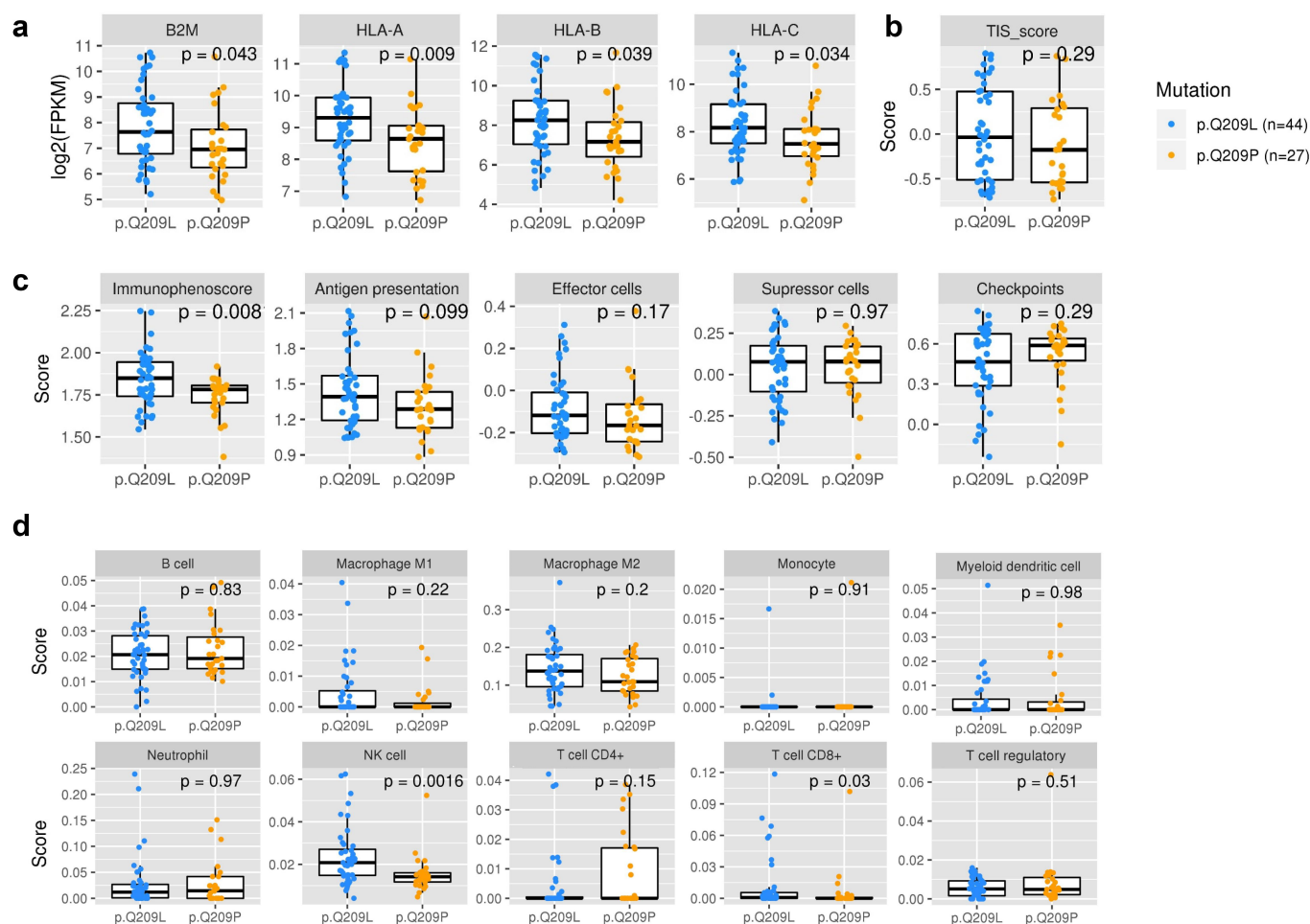


**Figure 7.** Characterization of immune state in patients carrying Q209L variant and Q209P variant. a) Levels of expression of antigen presenting genes B2M, HLA-A, HLA-B, and HLA-C. (b) T cell inflammatory signaling (TIS) score. c) Immunophenoscore (IPS), antigen presentation, effector cells, suppressor cells, and checkpoints scores. d) Immune cell infiltration. The Wilcoxon test was used to calculate statistically significant differences ( $p$ -value  $< 0.05$ ).

Q209L mutated patients ( $p = .0081$ ) (Figure 7c). This score is based on four sub-scores that represent the activation of antigen presentation, effector cells, suppressor cells, and checkpoint markers (neither of those showed statistically significant differences, although there is a tendency to higher antigen presentation and effector cell activation in Q209L patients).

To explore the infiltrate in detail, we used the Quantiseq method for estimating the infiltration of immune cells in the tumor microenvironment (Figure 7d). We found higher infiltration of T cells CD8+ ( $p = .03$ ) and NK cells ( $p = .0016$ ) in Q209L patients. To validate these results, we estimated the scores with a second method, called ConsensusTME (consensus tumor microenvironment) (Supplementary Figure S6). In agreement with the previous method, we found that patients carrying Q209L mutations tended to have higher infiltration scores for CD8 T cells ( $p = .065$ ). In contrast, we found no differences in NK cells. No differences were found for the other cell types with this method, although there was a trend toward higher scores of B cells in Q209P patients. Despite the variability between the methods, all results suggest a distinct immune microenvironment modulation, indicating a high

immune reactive phenotype in tumors harboring Q209L mutations.

Finally, to look at differences in activated biological pathways, a differential expression followed by gene-set enrichment analysis between Q209L carriers and Q209P carriers was performed. A total of 12 genes were found at  $p$ -values of  $< 0.05$  and absolute values of  $\log_{2}FC > 1$ , of which nine were overexpressed in Q209L patients and three were overexpressed in Q209P patients (Supplementary Table S8). In the functional analysis, as expected, most enriched gene sets for Q209L patients were related to the immune system (IFN- $\gamma$ ,  $p$ -adj =  $1.38e-12$ ; IFN- $\alpha$ ,  $p$ -adj =  $3.06e-8$ , IL6/JAK/STAT3,  $p$ -adj =  $1.4e-3$ ). Also, other pathways related to tumor growth and metabolism emerged (mTOR signaling,  $p$ -adj =  $5.16e-5$ ; hypoxia,  $p$ -adj =  $0.011$ , oxidative phosphorylation,  $p$ -adj =  $0.03$ , and fatty acid metabolism,  $p = .04$ ) (Supplementary Figure S7, Supplementary Table S9). Otherwise, there were not any pathways enriched in Q209P patients. This result suggests a crosstalk between immune infiltrate and other components of the tumor biology in Q209L carriers.

## 4. Discussion

Activating mutations in the Gαq signaling pathway at the level of GNAQ and GNA11 genes are considered alterations driving proliferation in UM. A great deal of research has been devoted to understanding molecular mechanisms behind these alterations, which transfer signaling from GPCRs to downstream effectors by activating the pathway constitutively. Also, to develop blocking drugs<sup>34</sup>. Despite these efforts, no novel treatment targeting this pathway has improved the prognosis of UM patients. Due to the exclusive immune microenvironment of UM, here we propose to study these driver mutations from an immunogenic point of view.

We hypothesize that different amino acids in the same position (P or L) activate a different immune response in the patient, rather than being GNAQ or GNA11 mutant. To the best of our knowledge, little is known about the differences between tumors harboring Q209P or Q209L mutations. Yet, a study by Maziarz et al showed fundamental differences in the molecular properties of Gq Q209P compared with proteins harboring Q209L, due to different structural conformations of the aberrant proteins.<sup>35</sup>

GNAQ/11 mutations appear in benign tumors and certain neoplasias. However, in malignant tumors, contrary to other driver mutations such as those in p53 or BRAF, among others, GNAQ and GNA11 are almost UM-exclusive mutations. Although marginal, other mutations including those in position Q209 have been described in skin melanoma and other tumors.<sup>36</sup> We mined 31 TCGA studies in cBioPortal<sup>16</sup> and only found 5 skin melanoma patients out of 10,887 patients harboring Q209P/L mutation. Other mutations apart from Q209 has been found in GNAQ/11 genes, but those are beyond this study. Several reasons may explain this addition for uveal melanoma. On the one hand, these alterations could help cancer cells to acquire an eye-specific adaptation. On the other hand, it might be hypothesized that tumoral cells harboring these mutations in other organs are destroyed by the immune system in early stages of the disease. In this regard, it has been reported that highly recurrent oncogenic mutations have poor HLA class I presentation.<sup>37</sup> Punta et al. reported that the median PMHBR of highly recurrent driver mutations in TCGA is 1.84, whereas the median PMHBR of passenger mutations in TCGA is 1.391. Thus, a driver mutation's frequency in cancer patients negatively correlates with the population's ability to present it.<sup>29,37</sup> Our results point to Q209L being more immunogenic than Q209P in 1000 G population. Despite being a driver mutation, it was more likely to be presented in comparison with other recurrent ones. In agreement, all tested tools except NetMHCpan predicted Q209L-derived peptide as highly immunogenic.

Neoantigens shared among groups of patients have become increasingly popular therapeutic targets. Obviously, non-recurrent, passenger mutations generating neoantigens need personalized logistics to be therapeutically exploited. On the contrary, public mutations simplify

all this process. In this regard, several public neoantigens from mutations in KRAS, BRAF, and TP53 genes have been described so far.<sup>15</sup> A recent work by Samuels et al. describing the combination of HLA-A\*01:01 and driver mutation RAS.Q61K as potentially immunogenic in 3% of melanoma patients is worth mentioning.<sup>38</sup>

We have found differences in immune system activation and infiltration between Q209L and Q209P tumors, being Q209L those scoring better in immunophenoscore. In agreement, Q209L tumors showed higher expression of genes related to antigen presentation. Interestingly, Q209L tumors showed higher infiltration of T-cells and NK cells. It has been reported that normal ocular cells express little or no MHC class I molecules to avoid recognition by cytotoxic T-cells. Aqueous humor or eye contains immunosuppressive factors inhibiting NK cells such as TGF-beta or MIF. Paradoxically, metastasizing cells in UM upregulate HLA molecules. Probably, this is because uveal melanoma cells with lower HLA expression are susceptible to being detected and eliminated by NK cells.<sup>39</sup> In agreement, *in vitro* studies have demonstrated the ability of cytotoxic NK cells to detect and kill uveal melanoma cells.<sup>40,41</sup>

Also, differences at the functional level have been found. Interestingly, Q209L score is better in pathways related to inflammation like interferon alpha and gamma response reinforcing those tumors to be more immunogenic. So, regarding immunotherapy response, one can hypothesize that those patients harboring Q209L mutation and appropriate HLA type would have a better outcome with immune checkpoint inhibitors (ICI). However, no changes in the inflammatory microenvironment or in HLA expression have been found in a similar study comparing Q209L vs. Q209P primary uveal tumors.<sup>42</sup>

Considering that eye is not entirely immuno-suppressed and based on the hypothesis that people presenting Q209L neoantigen are at lower risk of developing UM, one could expect HLA alleles to show low BR scores (meaning a high likelihood of the neoantigen to be presented by HLA) in the healthy population and HLA alleles to show high BR scores in UM patients. In agreement, some significant associations were observed between HLA genotypes and risk of suffering uveal melanoma. Also, we speculate that Q209L patients could be at lower risk of developing metastasis since the immune system recognizes tumoral cells out of the eye. However, no clear associations have been found between HLA haplotypes and survival in Q209L mutant patients. These suggest that the genetics of patients could impact directly disease initiation through Q209L presentation but not in progression, or at least there are other implicated factors. Interestingly, a negative correlation has been found between BR score and HLA-C frequency in both uveal patients and the general population, suggesting HLA-C as the best-presenting allele for this specific neoantigen. However, the low number of UM samples prevented us from accepting these observations and further investigation on independent datasets is needed.

In terms of prognosis, mutations in GNA11 have been moderately associated with poor prognosis and found more frequently in metastatic UM than GNAQ mutations.<sup>43,44</sup> Other

analysis, however, found no differences.<sup>42</sup> Looking at amino acidic changes, in TCGA-UM data, a marginal p-value of 0.06 pointed to Q209L being associated with a high risk of relapse. No differences in survival status were found. However, amid controversy, our results on an independent clinical dataset of primary UM samples showed Q209P patients having a trend toward poor prognosis (although not significant). Interestingly, Terai et al. identified that differences in mutation patterns (Q209P vs. Q209L) in GNAQ and GNA11, rather than GNAQ and GNA11 themselves, might predict the survival of metastatic UM patients. After the development of metastasis, patients with GNAQ Q209P mutant tumors had a more favorable outcome than patients with GNA11 Q209L and GNAQ Q209L mutant tumors.<sup>45</sup> It is also controversial, but in the primary tumor setting, a work by van Weeghel et al. found no differences in prognosis based on Q209P or L mutation but in Chromosome 3 status (monosomy or disomy), as previously reported.<sup>42</sup> In our data, there is no association between Chromosome 3 status and Q209P or L mutation.

This study has several limitations. It has not been validated in independent datasets because of scarce data about the amino acidic change in GNAQ and GNA11 mutations. Functional analysis comparing tumors harboring Q209P and Q209L could be biased by differences in number of samples between the two groups. Unfortunately, binding predictors do not perform well with HLA-II, so these genes' role deserves further study. Also, prediction binding algorithms could produce false-positive results. The limited sample size is also a drawback. Finally, the study is primarily computational.

Despite the shortcomings, it is worth mentioning that an existing patent (WO2019241666) validates our observations. It already defines a technology for the development of a vaccine to treat uveal melanoma based on GNAQ/GNA11 mutations. It shows how the binding of the mutated peptide FRMVDVGGL, which was also found in our study, is more immunogenic than the binding with wild-type peptide. Also, they describe that the critical amino acids for the binding were R in position 2 and Q/L in position 9, located in the MHC pocket acting as an anchor. Also in agreement with our results, a recent work by Gurung et al. looking for clinically actionable tumor neoantigens highlights Q209L mutation as a potential target. They identified unique neopeptide-HLA pairs running TR-FRET assays and then validated their immunogenicity using a mass spectrometry technology approach. Interestingly, the FRMVDVGGL peptide we selected as the most immunogenic was validated. Specifically, when presented by C×06:02 allele, that was also in agreement with our results.<sup>46</sup>

Treatment of UM continues to be a challenge, especially in metastatic patients. In this study, we provide bioinformatic evidence suggesting that GNAQ/GNA11 mutations can generate immunogenicity and we have proposed a potential candidate for a neoantigen vaccine targeting uveal melanoma. Next step is to modulate Q209L-HLA binding to in silico infer tentative therapeutic approaches based on blocking antibodies or vaccines, among others. Moreover, subsequent studies will be performed to experimentally demonstrate that Q209L mutation is presented in the MHC context and detected by T cells. Although

preliminary, our work paves the way for future therapeutic options in uveal melanoma patients.

## Acknowledgments

We thank CERCA Program, Generalitat de Catalunya for institutional support. We also thank the Consortium for Biomedical Research in Epidemiology and Public Health (CIBERESP).

## Disclosure statement

Dr Josep M Piulats has acted as a consultant or advisor for Roche, Novartis, Bristol Meyers Squibb, MSD Merck Serono, AstraZeneca, Clovis, VCN Biosciences, Janssen, Astellas, Bayer, Sanofi Genzyme, and Pfizer; received research funding from Pfizer, Merck Serono, MSD, Bristol Myers Squibb, Incyte, VCN Biosciences, Astellas, and Janssen; and received financial support for attending symposia from Roche, Janssen, and Ipsen.

## Funding

This work was supported by the Catalan Institute of Oncology, Aragon Government (Group B29\_23R), grupo Español Multidisciplinar de Melanoma (GEM), through the call "I Beca GEM al mejor proyecto GEM" and also has been funded by Instituto de Salud Carlos III through the grant [INT21/00056]. Sandra Garcia receives fund from PID2021-128343OB-I00 project from MCIN/AEI/10.13039/501100011033/FEDER, UE). We thank CERCA Programme/Generalitat de Catalunya for institutional support.

## Data availability statement

The data that support the findings of this study are openly available in TCGA repository.

## References

- Mallone S, De Vries E, Guzzo M, Midena E, Verne J, Coebergh JW, Marcos-Gragera R, Ardanaz E, Martinez R, Chirlaque MD, et al. Descriptive epidemiology of malignant mucosal and uveal melanomas and adnexal skin carcinomas in Europe. *Eur J Cancer*. 2012 May;48(8):1167–1175. doi:10.1016/j.ejca.2011.10.004.
- Yang J, Manson DK, Marr BP, Carvajal RD. Treatment of uveal melanoma: where are we now? *Ther Adv Med Oncol*. 2018;10:1758834018757175. doi:10.1177/1758834018757175.
- Nathan P, Hassel JC, Rutkowski P, Baurain JF, Butler MO, Schlaak M, Sullivan RJ, Ochsenreither S, Dummer R, Kirkwood JM, et al. Overall survival benefit with tebentafusp in metastatic uveal melanoma. *N Engl J Med*. 2021 Sep 23;385(13):1196–1206. doi:10.1056/NEJMoa2103485.
- Carvajal RD, Butler MO, Shoushtari AN, Hassel JC, Ikeguchi A, Hernandez-Aya L, Nathan P, Hamid O, Piulats JM, Rieth M, et al. Clinical and molecular response to tebentafusp in previously treated patients with metastatic uveal melanoma: a phase 2 trial. *Nat Med*. 2022 Nov;28(11):2364–2373. doi:10.1038/s41591-022-02015-7.
- Jager MJ, Shields CL, Cebulla CM, Abdel-Rahman MH, Grossniklaus HE, Stern MH, Carvajal RD, Belfort RN, Jia R, Shields JA, et al. Uveal melanoma. *Nat Rev Dis Primers*. 2020 Apr 9;6(1):24. doi:10.1038/s41572-020-0158-0.
- Park JJ, Diefenbach RJ, Joshua AM, Kefford RF, Carlino MS, Rizos H. Oncogenic signaling in uveal melanoma. *Pigment Cell Melanoma Res*. 2018 Nov;31(6):661–672. doi:10.1111/pcmr.12708.
- Shain AH, Bagger MM, Yu R, Chang D, Liu S, Vemula S, Weier JF, Wadt K, Heegaard S, Bastian BC, et al. The genetic evolution of metastatic uveal melanoma. *Nat Genet*. 2019 Jul;51(7):1123–1130. doi:10.1038/s41588-019-0440-9.

8. Piulats JM, Espinosa E, de la Cruz Merino L, Varela M, Alonso Carrión L, Martín-Algarra S, López Castro R, Curiel T, Rodríguez-Abreu D, Redrado M, et al. Nivolumab plus ipilimumab for treatment-naïve metastatic uveal melanoma: an open-label, multicenter, phase II trial by the Spanish Multidisciplinary melanoma group (GEM-1402). *J Clin Oncol*. 2021 Feb 20;39(6):586–598. doi:10.1200/JCO.20.00550.
9. Algazi AP, Tsai KK, Shoushtari AN, Munhoz RR, Eroglu Z, Piulats JM, Ott PA, Johnson DB, Hwang J, Daud AI, et al. Clinical outcomes in metastatic uveal melanoma treated with PD-1 and PD-L1 antibodies. *Cancer*. 2016 Nov 15;122(21):3344–3353. doi:10.1002/cncr.30258.
10. Niederkorn JY. Immune escape mechanisms of intraocular tumors. *Prog Retin Eye Res*. 2009 Sep;28(5):329–347. doi:10.1016/j.preteyres.2009.06.002.
11. Cross NA, Murray AK, Rennie IG, Ganesh A, Sisley K. Instability of microsatellites is an infrequent event in uveal melanoma. *Melanoma Res*. 2003 Oct;13(5):435–440. doi:10.1097/00008390-200310000-00001.
12. García-Mulero S, Alonso MH, Del Carpio LP, Sanz-Pamplona R, Piulats JM. Additive role of immune system infiltration and angiogenesis in uveal melanoma progression. *Int J Mol Sci*. 2021 Mar 6;22(5):2669. doi:10.3390/ijms22052669.
13. de la Cruz PO, Specht CS, McLean IW. Lymphocytic infiltration in uveal malignant melanoma. *Cancer*. 1990 Jan 1;65(1):112–115. doi:10.1002/1097-0142(19900101)65:1<112::AID-CNCR2820650123>3.0.CO;2-X.
14. Whelchel JC, Farah SE, McLean IW, Burnier MN. Immunohistochemistry of infiltrating lymphocytes in uveal malignant melanoma. *Invest Ophthalmol Visual Sci*. 1993 Jul;34(8):2603–2606.
15. Pearlman AH, Hwang MS, König MF, Hsiue EHC, Douglass J, DiNapoli SR, Mog BJ, Bettegowda C, Pardoll DM, Gabelli SB, et al. Targeting public neoantigens for cancer immunotherapy. *Nat Cancer*. 2021 May;2(5):487–497. doi:10.1038/s43018-021-00210-y.
16. Cerami E, Gao J, Dogrusoz U, Gross BE, Sumer SO, Aksoy BA, Jacobsen A, Byrne CJ, Heuer ML, Larsson E, et al. The cBio cancer genomics portal: an open platform for exploring multidimensional cancer genomics data. *Cancer Discov*. 2012 May;2(5):401–404. doi:10.1158/2159-8290.CD-12-0095.
17. Lundegaard C, Lamberth K, Harndahl M, Buus S, Lund O, Nielsen M. NetMHC-3.0: accurate web accessible predictions of human, mouse and monkey MHC class I affinities for peptides of length 8–11. *Nucleic Acids Res*. 2008 Jul 1;36(suppl\_2):W509–W512. doi:10.1093/nar/gkn202.
18. Reynisson B, Alvarez B, Paul S, Peters B, Nielsen M. NetMHCpan-4.1 and NetMHCIIpan-4.0: improved predictions of MHC antigen presentation by concurrent motif deconvolution and integration of MS MHC eluted ligand data. *Nucleic Acids Res*. 2020 Jul 2;48(W1):W449–54. doi:10.1093/nar/gkaa379.
19. Karosiene E, Lundegaard C, Lund O, Nielsen M. NetMHCcons: a consensus method for the major histocompatibility complex class I predictions. *Immunogenetics*. 2012 Mar;64(3):177–186. doi:10.1007/s00251-011-0579-8.
20. Phloyphisut P, Pornputtpong N, Sriswasdi S, Chuangsuwanich E. MHCSeqNet: a deep neural network model for universal MHC binding prediction. *BMC Bioinform*. 2019 May 28;20(1):270. doi:10.1186/s12859-019-2892-4.
21. O'Donnell TJ, Rubinsteyn A, Laserson U. Mhcflurry 2.0: improved Pan-allele prediction of MHC class I-Presented peptides by incorporating antigen processing. *Cell Syst*. 2020 Oct 21;11(4):418–419. doi:10.1016/j.cels.2020.09.001.
22. Nielsen M, Lundegaard C, Wornung P, Lauemøller SL, Lamberth K, Buus S, Brunak S, Lund O. Reliable prediction of T-cell epitopes using neural networks with novel sequence representations. *Protein Sci*. 2003 May;12(5):1007–1017. doi:10.1110/ps.0239403.
23. Andreatta M, Nielsen M. Gapped sequence alignment using artificial neural networks: application to the MHC class I system. *Bioinformatics*. 2016 Feb 15;32(4):511–517. doi:10.1093/bioinformatics/btv639.
24. Rasmussen M, Fenoy E, Harndahl M, Kristensen AB, Nielsen IK, Nielsen M, Buus S. Pan-specific prediction of peptide–MHC class I complex stability, a correlate of T cell immunogenicity. *J Immunol*. 2016 Aug 15;197(4):1517–1524. doi:10.4049/jimmunol.1600582.
25. Bassani-Sternberg M, Chong C, Guillaume P, Solleder M, Pak H, Gannon PO, Kandalaf LE, Coukos G, Gfeller D. Deciphering HLA-I motifs across HLA peptidomes improves neo-antigen predictions and identifies allosteric regulating HLA specificity. *PLoS Comput Biol*. 2017 Aug;13(8):e1005725. doi:10.1371/journal.pcbi.1005725.
26. Peters B, Bulik S, Tampe R, Van Endert PM, Holzhtüter HG. Identifying MHC class I epitopes by predicting the TAP transport efficiency of epitope precursors. *J Immunol*. 2003 Aug 15;171(4):1741–1749. doi:10.4049/jimmunol.171.4.1741.
27. Nielsen M, Lundegaard C, Lund O, Keşmir C. The role of the proteasome in generating cytotoxic T-cell epitopes: insights obtained from improved predictions of proteasomal cleavage. *Immunogenetics*. 2005 Apr;57(1–2):33–41. doi:10.1007/s00251-005-0781-7.
28. Fairley S, Lowy-Gallego E, Perry E, Flicek P. The International genome sample Resource (IGSR) collection of open human genomic variation resources. *Nucleic Acids Res*. 2020 Jan 8;48(D1):D941–7. doi:10.1093/nar/gkz836.
29. Punta M, Jennings VA, Melcher AA, Lise S. The immunogenic potential of recurrent cancer drug resistance mutations: an in silico study. *Front Immunol*. 2020;11:524968. doi:10.3389/fimmu.2020.524968.
30. Szolek A, Schubert B, Mohr C, Sturm M, Feldhahn M, Kohlbacher O. OptiType: precision HLA typing from next-generation sequencing data. *Bioinformatics*. 2014 Dec 1;30(23):3310–3316. doi:10.1093/bioinformatics/btu548.
31. Charoentong P, Finotello F, Angelova M, Mayer C, Efremova M, Rieder D, Hackl H, Trajanoski Z. Pan-cancer immunogenomic analyses reveal genotype-immunophenotype relationships and predictors of response to checkpoint blockade. *Cell Rep*. 2017 03;18(1):248–262. doi:10.1016/j.celrep.2016.12.019.
32. Hänzelmann S, Castelo R, Guinney J. GSVA: gene set variation analysis for microarray and RNA-seq data. *BMC Bioinform*. 2013 Jan 16;14(1):7. doi:10.1186/1471-2105-14-7.
33. Ayers M, Lunceford J, Nebozhyn M, Murphy E, Loboda A, Kaufman DR, Albright A, Cheng JD, Kang SP, Shankaran V, et al. IFN- $\gamma$ -related mRNA profile predicts clinical response to PD-1 blockade. *J Clin Invest*. 2017 Aug 1;127(8):2930–2940. doi:10.1172/JCI91190.
34. Ma J, Weng L, Bastian BC, Chen X. Functional characterization of uveal melanoma oncogenes. *Oncogene*. 2021 Jan;40(4):806–820. doi:10.1038/s41388-020-01569-5.
35. Maziarz M, Leyme A, Marivin A, Luebbers A, Patel PP, Chen Z, Sprang SR, Garcia-Marcos M. Atypical activation of the G protein G $\alpha_q$  by the oncogenic mutation Q209P. *J Biol Chem*. 2018 Dec 21;293(51):19586–19599. doi:10.1074/jbc.RA118.005291.
36. Larrière L, Utikal J. Update on GNA alterations in cancer: implications for uveal melanoma Treatment. *Cancers*. 2020 Jun 10;12(6):1524. doi:10.3390/cancers12061524.
37. Marty R, Kaabinejadian S, Rossell D, Slifker MJ, van de Haar J, Engin HB, de Prisco N, Ideker T, Hildebrand WH, Font-Burgada J, et al. MHC-I genotype restricts the oncogenic mutational landscape. *Cell*. 2017 Nov 30;171(6):1272–1283.e15. doi:10.1016/j.cell.2017.09.050.
38. Peri A, Greenstein E, Alon M, Pai JA, Dingjan T, Reich-Zeliger S, Barnea E, Barbolin C, Levy R, Arnedo-Pac C, et al. Combined presentation and immunogenicity analysis reveals a recurrent RAS.Q61K neoantigen in melanoma. *J Clin Invest*. 2021 Oct 15;131(20):e129466. doi:10.1172/JCI129466.
39. Javed A, Milhem M. Role of natural killer cells in uveal melanoma. *Cancers Basel*. 2020 Dec 9;12(12):E3694. doi:10.3390/cancers12123694.
40. Maat W, van der Slik AR, Verhoeven DHJ, Alizadeh BZ, Ly LV, Verduijn W, Luyten GPM, Mulder A, van Hall T, Koning F, et al. Evidence for natural killer cell-mediated protection from

- metastasis formation in uveal melanoma patients. *Invest Ophthalmol Visual Sci.* 2009 Jun;50(6):2888–2895. doi:[10.1167/iovs.08-2733](https://doi.org/10.1167/iovs.08-2733).
41. Ma D, Luyten GP, Luidert TM, Niederkorn JY. Relationship between natural killer cell susceptibility and metastasis of human uveal melanoma cells in a murine model. *Invest Ophthalmol Visual Sci.* 1995 Feb;36(2):435–441.
  42. van Weeghel C, Wierenga APA, Versluis M, van Hall T, van der Velden PA, Kroes WGM, Pfeffer U, Luyten GPM, Jager MJ. Do GNAQ and GNA11 differentially affect inflammation and HLA expression in uveal melanoma? *Cancers Basel.* 2019 Aug 7;11(8):E1127. doi:[10.3390/cancers11081127](https://doi.org/10.3390/cancers11081127).
  43. Griewank KG, van de Nes J, Schilling B, Moll I, Sucker A, Kakavand H, Haydu LE, Asher M, Zimmer L, Hillen U, et al. Genetic and clinico-pathologic analysis of metastatic uveal melanoma. *Mod Pathol.* 2014 Feb;27(2):175–183. doi:[10.1038/modpathol.2013.138](https://doi.org/10.1038/modpathol.2013.138).
  44. Bauer J, Kilic E, Vaarwater J, Bastian BC, Garbe C, de Klein A. Oncogenic GNAQ mutations are not correlated with disease-free survival in uveal melanoma. *Br J Cancer.* 2009 Sep 1;101(5):813–815. doi:[10.1038/sj.bjc.6605226](https://doi.org/10.1038/sj.bjc.6605226).
  45. Terai M, Shimada A, Chervoneva I, Hulse L, Danielson M, Swensen J, Orloff M, Wedegaertner PB, Benovic JL, Aplin AE, et al. Prognostic values of G-Protein mutations in metastatic uveal melanoma. *Cancers Basel.* 2021 Nov 17;13(22):5749. doi:[10.3390/cancers13225749](https://doi.org/10.3390/cancers13225749).
  46. Gurung H, Heidersbach A, Darwish M, Chan P, Li J, Beresini M, Zill O, Wallace A, Tong, AJ, Hascall, D, et al. Discovery of pre-valent, clinically actionable tumor neoepitopes via integrated biochemical and cell-based platforms [internet]. *Cancer Biology.* 2022 Oct; [accessed 2023 Jan 16]. doi:[10.1101/2022.10.27.513529](https://doi.org/10.1101/2022.10.27.513529).